Acta Crystallographica Section F
Structural Biology and Crystallization Communications
ISSN 1744-3091

Crystallization and preliminary X-ray diffraction analysis of the middle domain of Paip1

Ahmad Seif Kanaan,[a,b] Filipp Frank,[a,b,c] Chelsea Maedler-Kron,[a,b] Karan Verma,[a,b] Nahum Sonenberg[a,c] and Bhushan Nagar[a,b]*

[a]Department of Biochemistry, McGill University, Montréal, Québec, Canada, [b]Groupe de Recherche Axé sur La Structure des Protéines (GRASP), Montréal, Québec, Canada, and [c]Goodman Cancer Centre, McGill University, Montréal, Québec, Canada

Correspondence e-mail: bhushan.nagar@mcgill.ca

Received 20 July 2009
Accepted 9 September 2009

The poly(A)-binding protein (PABP) simultaneously interacts with the poly(A) tail of mRNAs and the scaffolding protein eIF4G to mediate mRNA circularization, resulting in stimulation of protein translation. PABP is regulated by the PABP-interacting protein Paip1. Paip1 is thought to act as a translational activator in 5′ cap-dependent translation by interacting with PABP and the initiation factors eIF4A and eIF3. Here, the crystallization and preliminary diffraction analysis of the middle domain of Paip1 (Paip1M), which produces crystals that diffract to a resolution of 2.2 Å, are presented.

1. Introduction

Eukaryotic translational control is critical for gene regulation during stress, development, differentiation, nervous-system function and disease (Sonenberg & Hinnebusch, 2009). Translation is initiated by the recruitment of several initiation factors (eIFs), including enzymes and adaptor/scaffolding proteins, that form (*via* a series of steps) a large complex that localizes the mRNA to be translated to the ribosome. Once assembled, the 43S pre-initiation complex, which includes the small ribosomal subunit, can scan along the mRNA to locate the translation-initiation codon and commence translation. Initiation is the most highly regulated and the rate-limiting step of translation and regulation can occur at multiple junctures along the process (Sonenberg & Hinnebusch, 2009). Proper regulation of this early step is essential, as abnormalities in the process can affect cell growth, proliferation and development, possibly leading to transformation (Schneider & Sonenberg, 2007).

A central facet of the formation of the initiation complex is the circularization of the mRNA, which has been shown to stimulate translational rates (Gallie, 1991; Munroe & Jacobson, 1990). Circularization is mediated by a bridging complex composed of the 5′ cap-bound eukaryotic translation initiation factor 4F (eIF4F) and the mRNA 3′ poly(A) tail-associated binding protein (PABP) (Kahvejian *et al.*, 2001). eIF4F is itself a three-subunit complex composed of the cap-binding protein eIF4E, the ATP-dependent RNA helicase eIF4A and the modular scaffolding protein eIF4G (Gingras *et al.*, 1999). The N-terminal region of eIF4G can simultaneously interact with both eIF4E and PABP, resulting in mRNA circularization (Imataka & Sonenberg, 1997; Tarun & Sachs, 1996). Several models have been put forward to explain how a closed-loop mRNA stimulates translation. One hypothesis suggests that a closed loop may promote the recycling of terminating ribosomes (Kahvejian *et al.*, 2001). Another possibility is that PABP stabilizes the eIF4F–cap interaction, thus stimulating 40S ribosomal binding (Kahvejian *et al.*, 2001). A third model proposes that PABP somehow increases 60S ribosomal joining (Kahvejian *et al.*, 2005). PABP is an essential multidomain protein that coats the poly(A) tail of mRNAs *via* interactions with its four phylogenetically conserved tandem RNA-recognition motifs (RRMs). These interactions are subject to regulation by the PABP-interacting proteins Paip1 and Paip2A/B (Craig *et al.*, 1998; Khaleghpour *et al.*, 2001).

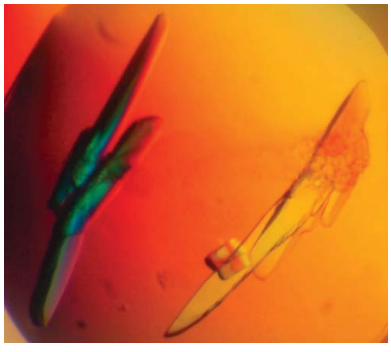

Human Paip1 is a 479-residue protein that occurs as three different isoforms arising owing to alternative splicing and promoter usage (Craig *et al.*, 1998). It is involved in the control of cell growth, proliferation and differentiation. Paip1 stimulates translation rates and has therefore been implicated in several pathogenic roles (Schneider & Sonenberg, 2007). It is overexpressed in invasive cervical cancers (Scotto *et al.*, 2008) and in amyotrophic lateral sclerosis (ALS; Fukada *et al.*, 2007).

The interaction between PABP and Paip1 is mediated by two separate PABP-binding motifs (PAM1 and PAM2) located at either end of Paip1 (Roy *et al.*, 2002). PAM1 is an acidic residue-rich region that spans residues 440–479 and binds to the N-terminal RRM2 region of PABP, whereas PAM2 spans residues 123–137 and binds to the C-terminal domain of PABP (PABC) (Kozlov *et al.*, 2004). The central region of Paip1 (residues 157–375) exhibits 21% sequence identity to the middle domain of eIF4G (MIF4G) and therefore may possess a similar structure. MIF4G is a HEAT domain consisting of five consecutive antiparallel helix–turn–helix motifs forming a right-handed superhelical structure (Marcotrigiano *et al.*, 2001). In eIF4G, this region harbours binding sites for both eIF4A and eIF3 (LeFebvre *et al.*, 2006; Imataka & Sonenberg, 1997). Immunoprecipitation experiments have suggested that Paip1 can also bind to eIF4A and eIF3 (Craig *et al.*, 1998; Martineau *et al.*, 2008). Thus, in a manner similar to eIF4G, Paip1 may also facilitate mRNA circularization, underscoring the importance of this feature of translation.

Little is known about how Paip1 activity is regulated other than that the Paip1–eIF3 interaction is bolstered upon activation of the Akt/mTOR and MAPK signalling pathways (Derry *et al.*, 2006). Thus, Paip1 may be the physical conduit between these signalling pathways and PABP activity and by extension translational rate stimulation. Because Paip1 can modulate translation rates and is a potential link to major signalling pathways, structural analysis will shed light on its role in mediating interactions within the translation-initiation complex and provide clues to the regions of Paip1 that are involved in recruiting eIF3 and eIF4A. Both the PAM1- and PAM2-interacting motifs are connected to the putative MIF4G domain of Paip1 (Paip1M) by flexible segments as revealed by secondary-structure analysis and will be likely to hinder crystallization of the full-length protein. Thus, here we report the crystallization and preliminary diffraction analysis of Paip1M.

2. Materials and methods

2.1. Construction of expression vectors for recombinant Paip1

Based on secondary-structure predictions that were made using the *PredictProtein* server (Rost *et al.*, 2004) on full-length Paip1, a construct encompassing the putative MIF4G domain (residues 157–375; hereafter called Paip1M) was amplified by PCR using the forward primer 5′-GAGGATGGATCCACTCTATCAGAATATGTTCAG-3′ and the reverse primer 5′-GACTCTGAATTCTTAACTTGACCGGAGTTCTACAAG-3′ and subcloned into the *Bam*HI and *Eco*RI restriction sites of the bacterial expression vector pProEX-HTb (Invitrogen), which produces a fusion protein containing a TEV (tobacco etch virus) protease-cleavable hexahistidine tag at its N-terminus. Owing to a cloning artifact, the construct contains an additional five amino acids (sequence GAMGS) at the N-terminus.

2.2. Expression and purification

Recombinant Paip1M plasmid was transformed into *Escherichia coli* strain BL21 Star (DE3) (Invitrogen) and grown overnight to produce starter culture, which was then used to inoculate 1 l cultures of LB medium supplemented with ampicillin (100 mg l^{-1}). Bacterial cultures were grown at 310 K until an OD_{600} of 0.6 was reached, at which point protein expression was induced by the addition of 1 m*M* isopropyl β-D-1-thiogalactopyranoside (IPTG) and growth was continued for an additional 4 h at 303 K. Bacteria were harvested by centrifugation at 3000 rev min^{-1} (2264*g*) for 15 min at 277 K and lysed by two passes through a French press (Avestin) in cold lysis buffer *A* (25 m*M* Tris–HCl pH 8.0, 500 m*M* NaCl, 5% glycerol and 10 m*M* imidazole). Cell debris was pelleted by centrifugation at 20 000 rev min^{-1} (48 384*g*) for 30 min at 277 K. Soluble protein was applied onto an Ni Sepharose 6 column (HisTrap FF column, GE Healthcare) equilibrated in buffer *A*. Bound protein was eluted with a linear gradient using buffer *B* (25 m*M* Tris–HCl pH 8.0, 500 m*M* NaCl, 5% glycerol and 500 m*M* imidazole) and fractions containing Paip1M were pooled and cleaved with approximately 1 mg TEV protease per 20 mg crude protein at 277 K while dialyzing overnight against 25 m*M* Tris–HCl pH 8.0, 500 m*M* NaCl, 0.5 m*M* DTT and 5% glycerol with a 3.5 kDa molecular-weight cutoff cellulose membrane. Cleaved protein was collected in the flowthrough of a second Ni column. The resulting sample was diluted 1:10 with a buffer containing 25 m*M* Tris–HCl pH 8.0 and 5% glycerol to reduce the salt concentration, loaded onto an ion-exchange column (HiTrap Q HP, GE Healthcare) and eluted with a linear salt gradient (50–500 m*M* NaCl). The protein was then concentrated and loaded onto a Superdex 75 gel-filtration column (10/300, GE Healthcare) equilibrated in 25 m*M* Tris–HCl pH 8.0, 200 m*M* NaCl and 5% glycerol. Paip1M fractions were pooled and concentrated for crystallization trials. Purified proteins were sent to the Centre for Biological Applications of Mass Spectrometry (CBAMS) at Concordia University to assess their mass and homogeneity.

2.3. Expression and purification of SeMet Paip1M

SeMet labelling was performed using the methionine-pathway inhibition procedure (Doublié, 1997). Paip1M BL21 (DE3) colonies were inoculated into 1 ml LB starter culture supplemented with 100 mg l^{-1} ampicillin. The culture was grown at 310 K for 8 h, which was followed by centrifugation at 3000 rev min^{-1} (2264*g*) for 5 min. Pellets were resuspended in 1 ml 1× M9 medium and then diluted into 100 ml 1× M9 medium treated with 100 mg l^{-1} ampicillin. The M9 culture was grown for 14–16 h, which was followed by a 10× dilution into 1 l 1× M9 medium supplemented with 5 g glucose, 100 ml 1 *M* $CaCl_2$, 1 ml 2 *M* $MgSO_4$, 2 mg biotin, 2 mg thiamine and 100 mg ampicillin per litre. Upon reaching an OD_{600} of 0.6, 100 mg l^{-1} Lys, Phe and Thr and 50 mg ml^{-1} Ile, Leu, Val and SeMet were added. The cultures were induced with IPTG at a final concentration of 0.8 m*M*, at which point the temperature was lowered to 303 K and sustained for 4 h to facilitate protein expression. The cultures were harvested by centrifugation for 15 min at 3000 rev min^{-1} (2264*g*). The supernatant was discarded and the pellets were resuspended in 20–30 ml buffer *A*. SeMet-incorporated protein was purified as described above.

2.4. Crystallization and diffraction data collection

Protein crystallization was conducted at concentrations of 15 and 25 mg ml^{-1}. Initial screens were set up using the sitting-drop vapour-diffusion method (100 nl protein solution mixed with 100 nl crystallization condition) on Intelli-Plate 96-2 plates (Art Robbins) utilizing a Phoenix Crystallization Robot (Art Robbins). The Classics I, Classics II, Sparse Matrix I, Sparse Matrix II and PEG/Ion crystallization suites (Qiagen) were screened for initial trials. The drops were sealed with clear sealing tape and allowed to equilibrate against

Table 1
Data-collection statistics for Paip1M crystals.

Values in parentheses are for the highest resolution shell (2.28–2.20 Å).

No. of crystals	1
Wavelength (Å)	1.54
Crystal-to-detector distance (mm)	200
Oscillation width (°)	0.5
Exposure time (min)	6
No. of images collected	720
Resolution (Å)	2.20
Space group	$P2_1$
Unit-cell parameters (Å, °)	a = 58.8, b = 76.5, c = 62.3, α = 90.0, β = 96.1, γ = 90.0
No. of observations	178759
No. of unique reflections	25466
Mosaicity (°)	1.2
$R_{\rm merge}$† (%)	4.7 (18.2)
Completeness (%)	90.9 (56.4)
Mean $I/\sigma(I)$	32.3 (9.0)
Redundancy	7.0 (5.0)

† $R_{\rm merge} = \sum_{hkl}\sum_i |I_i(hkl) - \langle I(hkl)\rangle| / \sum_{hkl}\sum_i I_i(hkl)$, where $I_i(hkl)$ is the observed intensity for a reflection and $\langle I(hkl)\rangle$ is the average intensity obtained from multiple observations of symmetry-related reflections.

100 µl reservoir solution. Conditions that produced potential protein crystals were reproduced and optimized in grid screens surrounding the crystallization hits using the traditional hanging-drop vapour-diffusion technique with 1–2 µl drops equilibrated against 1 ml reservoir solution in 24-well EasyXtal tool plates (Qiagen). All crystallization experiments were carried out at room temperature (~295 K). Protein crystals were cryoprotected and flash-cooled in a liquid-nitrogen cold stream. Diffraction data were collected using a Rigaku rotating copper-anode generator fitted with Osmic confocal optics and an R-AXIS IV^{++} image-plate detector. Diffraction data were processed using *HKL*-2000 (Otwinowski & Minor, 1997).

3. Results and discussion

Recombinant Paip1M was overexpressed in *E. coli* and purified to homogeneity, yielding approximately 5 mg protein per litre of bacterial culture. SDS–PAGE indicated that the protein ran as an ~25 kDa band that was greater than 95% pure (Fig. 1, inset). Electrospray mass spectrometry revealed a mass of 25 366 Da, which agrees well with the calculated mass of 25 368 Da for the amino-acid sequence (Fig. 2*a*). Gel-filtration analysis resulted in a single symmetric peak centred around a retention volume that corresponds to a molecular weight of ~34 kDa (Fig. 1). This discrepancy in size can be explained by the fact that the MIF4G domain has an elongated shape (Marcotrigiano *et al.*, 2001), which probably causes it to elute from the gel-filtration column at a higher than expected molecular weight. Thus, Paip1M is likely to exist as a monomer in solution.

Of ~500 different crystallization conditions tested, three conditions produced what appeared to be protein crystals: (i) 20%(*w*/*v*) PEG 3350, 0.2 *M* $CaCl_2$, (ii) 15%(*w*/*v*) PEG 20 000, 0.1 *M* MES pH 6.5 and (iii) 17%(*w*/*v*) PEG 10 000, 0.1 *M* bis-tris pH 5.5, 0.1 *M* ammonium acetate (Fig. 3). All three conditions were reproduced and optimized in larger drops using the hanging-drop vapour-diffusion technique. In all cases, the crystals grew as fused clusters and had to be manually pried apart for data collection. Once isolated, single crystals were cryoprotected in a stepwise manner by increasing the existing glycerol concentration in the drop from 5% to 25% in 5% increments with an ~90 s soaking interval between each step. The cryoprotected crystals were then either flash-cooled in a liquid-nitrogen stream for immediate data collection or placed in a liquid-nitrogen dewar for storage. We proceeded further only with condition (ii), as it gave the best crystals based on preliminary diffraction analysis. The final optimized crystallization condition was 22%(*w*/*v*) PEG 20 000, 0.1 *M* MES pH 6.5 using a protein concentration of 25 mg ml^{-1}.

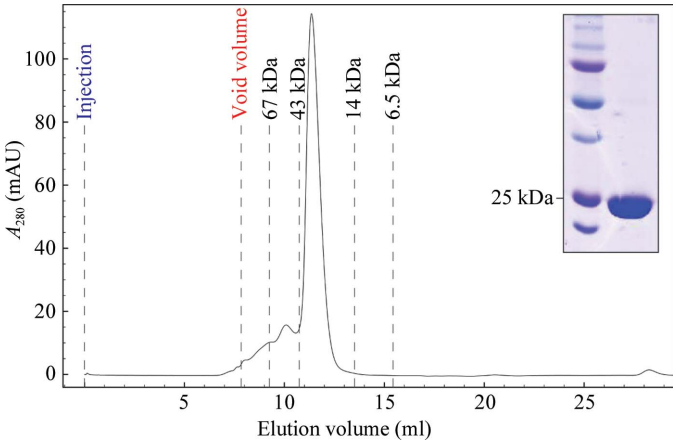

Figure 1
Analytical gel-filtration profile and SDS–PAGE analysis (inset) of purified Paip1M. Gel filtration was carried out on a 24 ml Superdex 75 column (GE Healthcare) which has a cutoff of 70 kDa and a void volume of ~8 ml. Vertical lines indicate the positions of molecular-weight standards. The shoulder to the left of the main peak indicates higher molecular-weight species that were omitted from the final pool. SDS–PAGE was carried out on a 12% polyacrylamide gel and the bands were visualized by Coomassie staining. Lane 1 contains molecular-weight markers (kDa) and lane 2 contains the purified recombinant Paip1M protein.

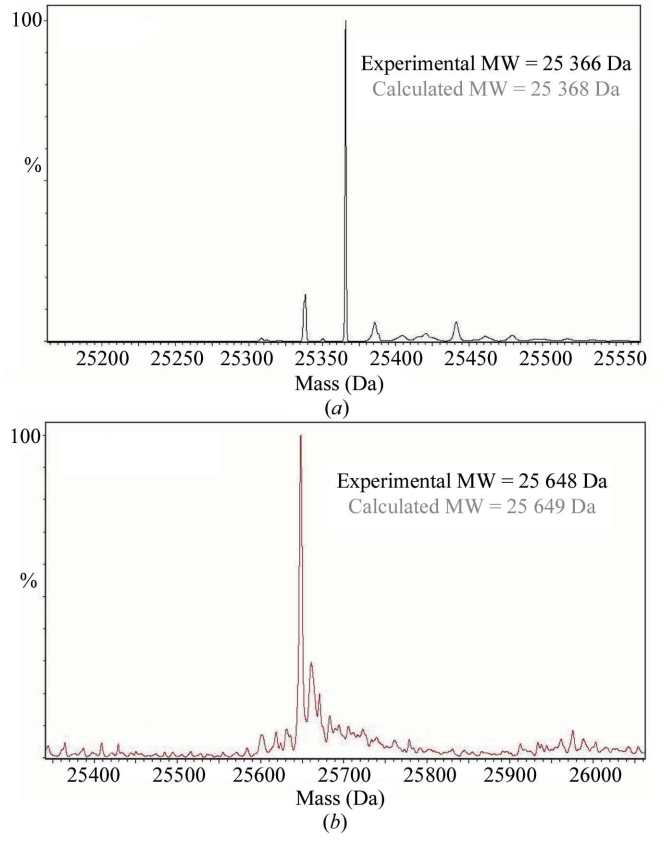

Figure 2
Mass-spectrometric analysis of purified (*a*) native Paip1M and (*b*) SeMet Paip1M. The increase in mass of the SeMet protein arises from the substitution of six Met residues with SeMet.

The crystals belonged to the monoclinic space group $P2_1$ and diffracted X-rays to beyond 2.2 Å resolution (Table 1 and Fig. 4). Matthews coefficient (V_M) analysis indicated that there were most likely to be two molecules in the asymmetric unit, resulting in a solvent content of ~55% and a V_M of 2.75 Å^3 Da^{-1} (Matthews, 1968). Since this region of Paip1 has been identified as a putative MIF4G domain, we attempted to solve the structure by molecular replacement using the crystal structure of the MIF4G domain of eIF4G (PDB code 1hu3, chain *A*; Marcotrigiano *et al.*, 2001) as a search model in the program *Phaser* (McCoy *et al.*, 2007). Unfortunately, this did not yield any obvious solutions.

There is only 21% sequence identity between eIF4G and Paip1M, indicating that there may be significant structural differences and that this may be a borderline case for the molecular-replacement technique. Self-rotation function analysis did not reveal the presence of any noncrystallographic twofold rotational symmetry. However, inspection of the native Patterson map revealed a 25σ non-origin peak at u = 0.42, v = 0.5, w = 0.06, indicating the presence of translational symmetry within the unit cell (Fig. 5). Thus, one possibility is that the two molecules in the asymmetric unit may be related by a pure translation. Alternatively, since the peak is on the Harker section, the two molecules may be related by a twofold noncrystallographic rotation axis that is coincident with the crystallographic twofold. This situation may make a molecular-replacement solution even more difficult, especially considering the low sequence identity between Paip1M and the search model; therefore, experimental

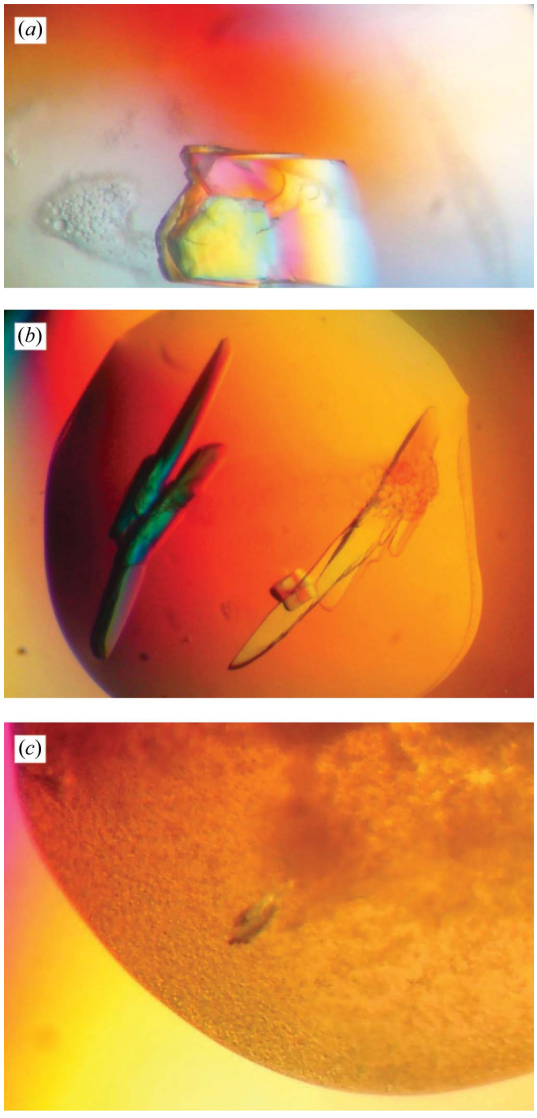

Figure 3
Paip1M crystals grown in (*a*) condition (i), (*b*) condition (ii) and (*c*) condition (iii) (see text for details). Only the crystals shown in (*b*) were used for subsequent diffraction analysis. These crystals were approximately 500 µm in the longest dimension.

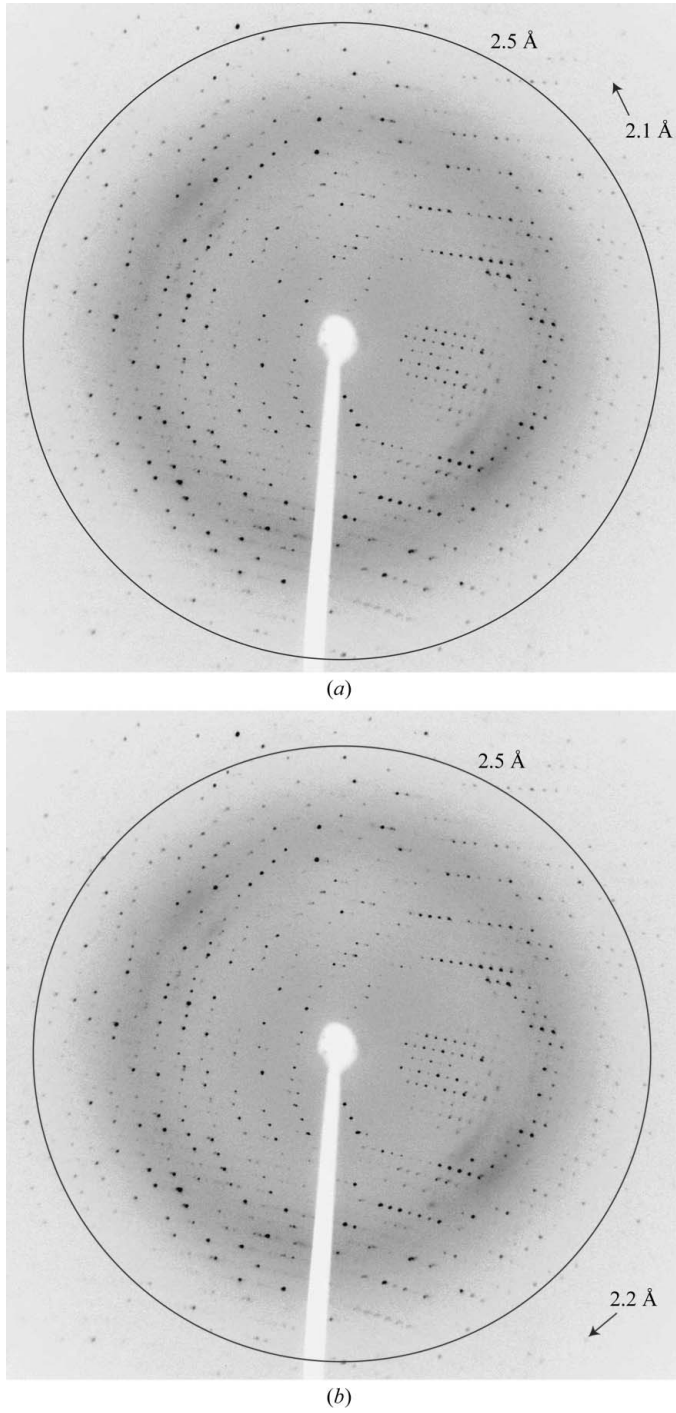

Figure 4
Representative X-ray diffraction patterns of Paip1M obtained on a home rotating-anode source. Black circles denote a resolution of 2.5 Å. High-resolution spots are indicated by arrows. Panels (*a*) and (*b*) are approximately 90° apart in reciprocal space.

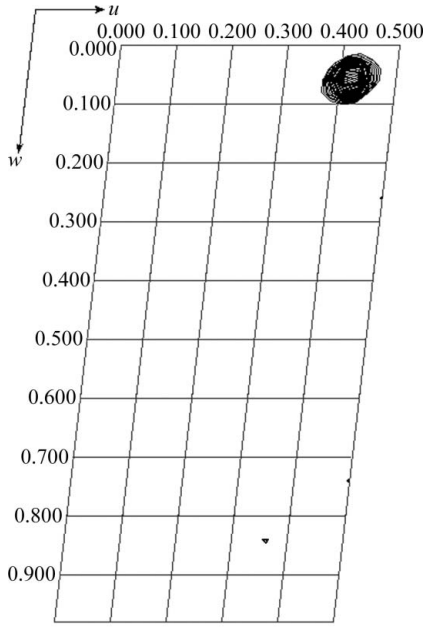

Figure 5
Harker section (v = 0.5) from the native Patterson function of the Paip1M diffraction data. The map was calculated using data between 50 and 4 Å resolution and is contoured in steps of 1σ beginning at 3σ above the mean.

phases will instead be determined. The multiwavelength anomalous dispersion (MAD) technique (Hendrickson, 1991) will be used with SeMet-substituted crystals since there are six methionine residues in Paip1M, which should provide a sufficient anomalous signal even with partial SeMet incorporation.

SeMet labelling was performed using the methionine-pathway inhibition procedure (Doublié, 1997). A yield similar to the wild-type purification (∼5 mg protein per litre of culture) was obtained of SeMet-labelled Paip1M. The mass difference for the substitution of six Met residues by SeMet is expected to be ∼281 Da. Mass-spectrometric analysis of SeMet Paip1M indicated that there was near full incorporation of SeMet within the protein (Fig. 4*b*). The SeMet-substituted protein crystallized in 19–22%(*w*/*v*) PEG 20 000, 0.1 *M* MES pH 6.5 and the crystals were similar in both size and shape to the wild-type crystals. MAD/SAD data-collection experiments will be performed on these crystals at a synchrotron source. The crystal structure of the middle domain of Paip1 will help to clarify its contribution to mRNA circularization in the translation-initiation complex and its potential interactions with eIF4A and eIF3.

This work was supported by a Career Development Award to BN from the Human Frontiers Science Program (CDA 0018/2006-C/1) and an operating grant from the Canadian Institutes of Health Research (CIHR grant MOP-82929). FF was supported by a Boehringer Ingelheim Fonds PhD fellowship. We thank Lama Talje, Yazan Abbas and Yvan Martineau for helpful discussions and Rose Szittner for technical support.

References

Craig, A. W., Haghighat, A., Yu, A. T. & Sonenberg, N. (1998). *Nature (London)*, **392**, 520–523.
Derry, M. C., Yanagiya, A., Martineau, Y. & Sonenberg, N. (2006). *Cold Spring Harb. Symp. Quant. Biol.* **71**, 537–543.
Doublié, S. (1997). *Methods Enzymol.* **276**, 523–530.
Fukada, Y., Yasui, K., Kitayama, M., Doi, K., Nakano, T., Watanabe, Y. & Nakashima, K. (2007). *Brain Res.* **1160**, 1–10.
Gallie, D. R. (1991). *Genes Dev.* **5**, 2108–2116.
Gingras, A. C., Raught, B. & Sonenberg, N. (1999). *Annu. Rev. Biochem.* **68**, 913–963.
Hendrickson, W. A. (1991). *Science*, **254**, 51–58.
Imataka, H. & Sonenberg, N. (1997). *Mol. Cell. Biol.* **17**, 6940–6947.
Kahvejian, A., Roy, G. & Sonenberg, N. (2001). *Cold Spring Harb. Symp. Quant. Biol.* **66**, 293–300.
Kahvejian, A., Svitkin, Y. V., Sukarieh, R., M'Boutchou, M. N. & Sonenberg, N. (2005). *Genes Dev.* **19**, 104–113.
Khaleghpour, K., Kahvejian, A., De Crescenzo, G., Roy, G., Svitkin, Y. V., Imataka, H., O'Connor-McCourt, M. & Sonenberg, N. (2001). *Mol. Cell. Biol.* **21**, 5200–5213.
Kozlov, G., De Crescenzo, G., Lim, N. S., Siddiqui, N., Fantus, D., Kahvejian, A., Trempe, J. F., Elias, D., Ekiel, I., Sonenberg, N., O'Connor-McCourt, M. & Gehring, K. (2004). *EMBO J.* **23**, 272–281.
LeFebvre, A. K., Korneeva, N. L., Trutschl, M., Cvek, U., Duzan, R. D., Bradley, C. A., Hershey, J. W. & Rhoads, R. E. (2006). *J. Biol. Chem.* **281**, 22917–22932.
Marcotrigiano, J., Lomakin, I. B., Sonenberg, N., Pestova, T. V., Hellen, C. U. & Burley, S. K. (2001). *Mol. Cell*, **7**, 193–203.
Martineau, Y., Derry, M. C., Wang, X., Yanagiya, A., Berlanga, J. J., Shyu, A. B., Imataka, H., Gehring, K. & Sonenberg, N. (2008). *Mol. Cell. Biol.* **28**, 6658–6667.
Matthews, B. W. (1968). *J. Mol. Biol.* **33**, 491–497.
McCoy, A. J., Grosse-Kunstleve, R. W., Adams, P. D., Winn, M. D., Storoni, L. C. & Read, R. J. (2007). *J. Appl. Cryst.* **40**, 658–674.
Munroe, D. & Jacobson, A. (1990). *Mol. Cell. Biol.* **10**, 3441–3455.
Otwinowski, Z. & Minor, W. (1997). *Methods Enzymol.* **276**, 307–326.
Rost, B., Yachdav, G. & Liu, J. (2004). *Nucleic Acids Res.* **32**, W321–W326.
Roy, G., De Crescenzo, G., Khaleghpour, K., Kahvejian, A., O'Connor-McCourt, M. & Sonenberg, N. (2002). *Mol. Cell. Biol.* **22**, 3769–3782.
Schneider, R. J. & Sonenberg, N. (2007). *Translational Control in Biology and Medicine*, edited by M. B. Mathews, N. Sonenberg & J. W. B. Hershey. New York: Cold Spring Harbor Laboratory Press.
Scotto, L., Narayan, G., Nandula, S. V., Subramaniyam, S., Kaufmann, A. M., Wright, J. D., Pothuri, B., Mansukhani, M., Schneider, A., Arias-Pulido, H. & Murty, V. V. (2008). *Mol. Cancer*, **7**, 58.
Sonenberg, N. & Hinnebusch, A. G. (2009). *Cell*, **136**, 731–745.
Tarun, S. Z. Jr & Sachs, A. B. (1996). *EMBO J.* **15**, 7168–7177.